

Cite this: *RSC Adv.*, 2018, 8, 33325

## Green and efficient biosynthesis of indigo from indole by engineered myoglobins†

Can Liu,<sup>‡a</sup> Jiakun Xu,<sup>‡b</sup> Shu-Qin Gao,<sup>‡c</sup> Bo He,<sup>a</sup> Chuan-Wan Wei,<sup>\*a</sup> Xiao-Juan Wang,<sup>a</sup> Zhonghua Wang<sup>d</sup> and Ying-Wu Lin<sup>ID \*ac</sup>

With the demand nowadays for blue dyes, it is of practical importance to develop a green and efficient biocatalyst for the production of indigo. The design of artificial enzymes has been shown to be attractive in recent years. In a previous study, we engineered a single mutant of sperm whale myoglobin, F43Y Mb, with a novel Tyr-heme cross-link. In this study, we found that it can efficiently catalyze the oxidation of indole to indigo, with a yield as high as 54% compared to the highest yield (~20%) reported to date in the literature. By further modifying the heme active site, we engineered a double mutant of F43Y/H64D Mb, which exhibited the highest catalytic efficiency ( $198 \text{ M}^{-1} \text{ s}^{-1}$ ) among the artificial enzymes designed in Mb. Moreover, both F43Y Mb and F43Y/H64D Mb were found to produce the indigo product with a chemoselectivity as high as ~80%. Based on the reaction system, we also established a convenient and green dyeing method by dyeing a cotton textile during the biosynthesis of indigo, followed by further spraying the concentrated indigo, without the need of strong acids/bases or any reducing agents. The successful application of dyeing a white cotton textile with a blue color further indicates that the designed enzyme and the dyeing method have practical applications in the future.

Received 20th September 2018

Accepted 21st September 2018

DOI: 10.1039/c8ra07825d

rsc.li/rsc-advances

## Introduction

The old textile dye indigo has been used for thousands of years, and is still in demand nowadays for dyeing cotton and wood fabrics, such as the most popular blue jeans.<sup>1,2</sup> Although it can be extracted from plants, synthetic indigo accounts for the main part of the market. As of 2011, worldwide production of denim used more than 95% of the 50 000 tons of synthetic indigo produced per year.<sup>3</sup> Meanwhile, from the view point of green chemistry, general organic synthesis has significant drawbacks, such as the demand of high energy, the use of organic solvents, and the production of toxic waste products.<sup>4</sup>

As an alternative approach, biosynthesis of indigo has been tested for decades. In 1983, Ensley *et al.* first constructed an *E. coli* strain encoding a naphthalene dioxygenase with coenzymes, which catalyzed synthesis of indigo from indole.<sup>1</sup> Later on, other biocatalysts of recombinant *E. coli* cells were

constructed by using engineered cytochrome P450s (CYP450s) with their cofactors such as NAD(P)H.<sup>5–8</sup> Meanwhile, the catalytic system was complicated and it was also difficult to obtain pure indigo from the culture media.<sup>8</sup> Moreover, the use of CYP450s *in vitro* requires the expensive cofactors of NAD(P)H,<sup>6–8</sup> which makes it not suitable for the practical production of indigo.

A small heme protein, myoglobin (Mb), has been shown to be favourable for design of artificial enzymes.<sup>9–22</sup> To develop a simple and economical approach to producing indigo from indole, Watanabe and co-workers constructed a  $\text{H}_2\text{O}_2$ -dependent catalytic oxidation system using Mb by replacement of the distal histidine (His64) with an aspartate, as well as other modifications in the heme distal pocket.<sup>23</sup> Unfortunately, the best indigo yield obtained was only 12%, based on the consumed indole.<sup>23</sup> Recently, Rebelo and co-workers developed an enzymatic mimicking system based on an Fe(III)-porphyrin that requires ethanol as a solvent. However, the indigo yield was still quite low (20%).<sup>24</sup> Therefore, it is of practical importance to develop a green and efficient biocatalyst for the production of indigo.

More recently, Dueber and co-workers reported a new strategy for dyeing by co-expressing a glucosyltransferase and a flavin-dependent monooxygenase in *E. coli*, which produces up to  $2.9 \text{ g L}^{-1}$  indican *in vivo* from fed tryptophan.<sup>25</sup> While the biosynthesized indican was successfully used as a textile dye, the incorporation of indican into a dye has practical challenges, such as the need of an enzyme or strong acid for hydrolysis, which requires further improvements.<sup>25</sup>

<sup>a</sup>School of Chemistry and Chemical Engineering, University of South China, Hengyang 421001, China. E-mail: linlinying@hotmail.com; ywlin@usc.edu.cn; Weichw@hotmail.com

<sup>b</sup>Yellow Sea Fisheries Research Institute, Qingdao 266071, China

<sup>c</sup>Laboratory of Protein Structure and Function, University of South China, Hengyang 421001, China

<sup>d</sup>College of Chemistry and Chemical Engineering, China West Normal University, Nanchong 637002, China

† Electronic supplementary information (ESI) available: ESI-MS, TLC and HPLC analysis, UV-Vis spectra and reaction mechanism. See DOI: 10.1039/c8ra07825d

‡ These authors contributed equally.

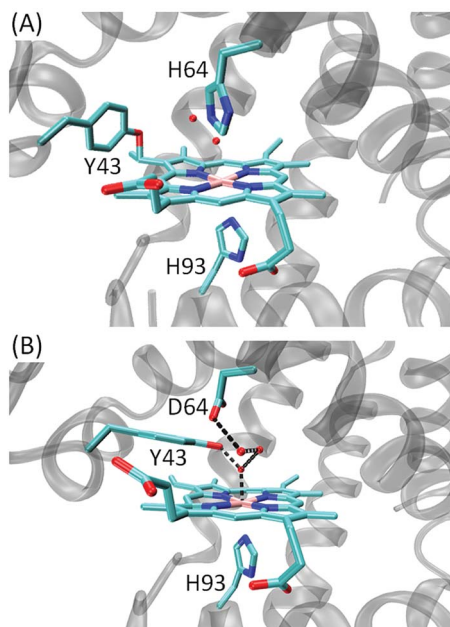


Fig. 1 X-ray structure of (A) F43Y Mb (PDB code 4QAU<sup>26</sup>) and (B) F43Y/H64D (PDB code 5ZZF<sup>29</sup>), showing the heme active site.

Motivated by these achievements, we were interested in engineering an enzyme capable of efficiently catalyzing the oxidation of indole to indigo. As demonstrated by Watanabe and co-workers, it is a simple and economical approach to design of artificial enzymes in Mb, despite with a low yield.<sup>23</sup> Therefore, we focused on the scaffold of Mb and attempted to further modify the heme active site. In a recent study, we discovered a novel Tyr-heme cross-link in F43Y Mb mutant, with an enhanced protein stability due to the non-dissociable heme group (Fig. 1A).<sup>26</sup> More importantly, F43Y Mb exhibited a dramatically increased ability (~100-fold) in activation of H<sub>2</sub>O<sub>2</sub> compared with that of wild-type (WT) Mb,<sup>26</sup> which provides an ideal protein scaffold for heme protein design.<sup>27,28</sup> We thus speculated that F43Y Mb may exhibit an activity towards the H<sub>2</sub>O<sub>2</sub>-dependent oxidation of indole. Moreover, we engineered a double mutant of F43Y/H64D Mb by replacing the distal His64 with an Asp (Fig. 1B),<sup>29</sup> as inspired by previous study on the single mutant of H64D Mb by Watanabe and co-workers.<sup>23</sup> As shown in this study, both F43Y Mb and F43Y/H64D Mb were capable of efficient biosynthesis of indigo from indole, with a high yield and chemoselectivity. In addition, the biosynthesized indigo in the reaction system was successfully used to dye cotton swatches, without the addition of acids/bases or any reducing agents.

## Results and discussion

### Indole oxidation and indigo formation

F43Y Mb was expressed and purified as our previously reported.<sup>26</sup> We first tested the oxidation of indole catalyzed by F43Y Mb using H<sub>2</sub>O<sub>2</sub> as an oxidant. As shown in Fig. 2A, when indole was mixed with F43Y Mb and followed by an addition of

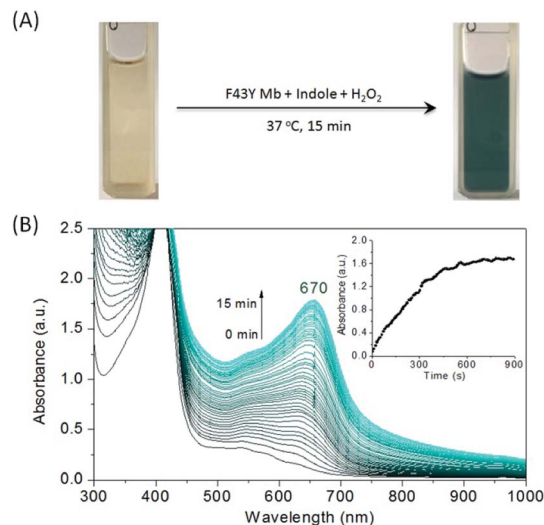


Fig. 2 (A) Color changes of the oxidation of indole (1 mM) catalyzed by F43Y Mb (20 μM) with H<sub>2</sub>O<sub>2</sub> (1 mM) as an oxidant. (B) UV-vis spectral changes of the oxidation of indole catalyzed by F43Y Mb. The change of the absorbance at 670 nm was shown as an inset.

H<sub>2</sub>O<sub>2</sub>, the color of the mixture gradually transformed into dark blue within 15 min, which indicated the oxidation of indole that likely produced indigo. We then monitored the UV-Vis spectral changes during the reaction, which showed a gradual increase of the absorbance with a maximum at 670 nm (Fig. 2B). We also optimized the reaction conditions by varying the concentrations of both indole and H<sub>2</sub>O<sub>2</sub> (Fig. S1†). It was shown that as catalyzed by 10 μM F43Y Mb, the yield could not be further improved by addition of more than 4 mM indole, and the increase of H<sub>2</sub>O<sub>2</sub> concentration more than 1 mM may cause an inhibition effect. Moreover, although indigo has a low solubility in water, we found that the biosynthesized indigo was well dispersed in the reaction solution, which produced blue precipitates by centrifugation. After re-dissolved in dimethylformamide (DMF), a transparent blue solution was obtained (Fig. 3A). As shown in Fig. 3B, the UV-Vis spectrum of this blue precipitate-DMF solution is consistent with the authentic indigo-DMF solution, with a distinct absorption peak at 610 nm, which initially confirms the product to be indigo.

In order to further verify the composition of the blue precipitate, we tested by both mass spectrometry and thin layer chromatography (TLC). The mass spectrum of the blue product showed a major peak at  $m/z$  261.07 [M-H]<sup>−</sup> that agrees well with the calculated mass for indigo (C<sub>16</sub>H<sub>10</sub>N<sub>2</sub>O<sub>2</sub>, 262.1), with a trace amount of side product, 6*H*-oxazolo[3,2-*a*:4,5-*b'*] diindole (C<sub>16</sub>H<sub>10</sub>N<sub>2</sub>O, 246.1) (Fig. S2†). Moreover, blue dots were observed in TLC by naked eye in daily light, and only these dots were observed with the UV lamp at 254 nm (Fig. S3†). These observations thus confirm that the blue precipitate obtained by centrifugation was indigo. Moreover, these results indicate that indigo with a high purity can be obtained simply by centrifugation of the reaction solution, without the use of any other chemicals.

As mentioned in Introduction, Watanabe and co-workers have constructed some artificial metalloenzymes capable of



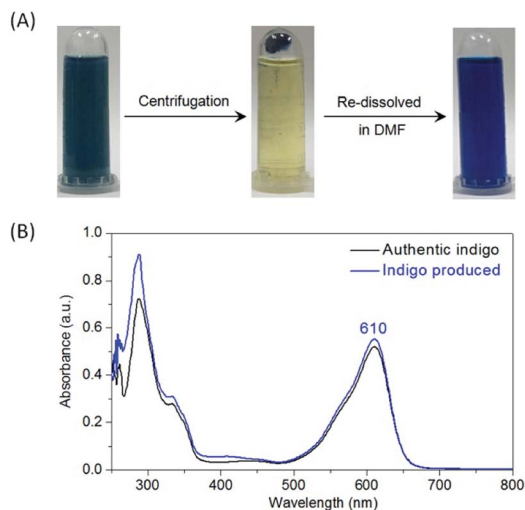


Fig. 3 (A) The reaction solution after indole oxidation catalyzed by F43Y Mb as shown in Fig. 1A, which produces blue precipitates after centrifugation, and generates a transparent blue solution by re-dissolving in DMF. (B) UV-visible spectral comparison between the bio-synthesized indigo (blue) and the authentic indigo (black).

producing indigo by oxidation of indole, by replacing the distal His64 of Mb with an Asp (H64D mutation) that facilitates indole binding to the heme active site, as well as other mutations.<sup>23</sup> Inspired by their design, we constructed a double mutant of F43Y/H64D Mb. Meanwhile, our recent X-ray crystallographic study showed that the Tyr-heme cross-link was not formed in this double mutant. Instead, Tyr43 interacted with the heme axial water, and Asp64 formed an H-bond network with several water molecules in the heme distal pocket (Fig. 1B).<sup>29</sup> We then tested the oxidation of indole catalyzed by this double mutant. As shown in Fig. S4,<sup>†</sup> the reaction solution turned to blue after 15 min, but the color was slightly lighter than that of catalyzed by F43Y Mb under the same conditions. The UV-Vis spectral changes showed that the final absorbance at 670 nm ( $A_{670\text{nm}} = \sim 1.2$ ) has a lower intensity compared to that of catalyzed by F43Y Mb ( $A_{670\text{nm}} = \sim 1.6$ ), indicating that less indigo was produced, albeit with the same initial concentration of indole. Control study using WT Mb showed that no product of indigo was produced, since no color or spectral changes were observed for the reaction solution (Fig. S5<sup>†</sup>). These observations suggest that modification of the heme active site of Mb can convert it into an enzyme catalyzing indole to form indigo.

### Kinetic studies of indigo formation

In order to determine the kinetic parameters for the formation of indigo, we performed kinetic UV-Vis studies by varying the concentrations of indole and monitoring the spectral changes at 670 nm in oxidation reaction. The plots of  $k_{\text{obs}}$  and the concentration of indole were fitted to the Michaelis-Menten equation (Fig. 4), and the obtained parameters,  $k_{\text{cat}}$  and  $K_{\text{m}}$ , were listed in Table 1. Note that the parameters can not be determined for WT Mb. The results showed that F43Y Mb exhibited a  $k_{\text{cat}}$  value ( $13.8 \text{ min}^{-1}$ )  $\sim 2.6$ -fold that of F43Y/H64D Mb, suggesting that the native distal His64 plays a crucial role

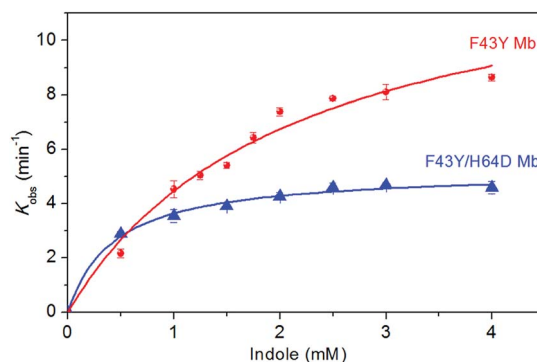


Fig. 4 The plots of catalytic reaction rates of the indigo formation as a function of indole concentrations, as catalyzed by F43Y Mb and F43Y/H64D Mb using  $\text{H}_2\text{O}_2$  as an oxidant in three experiments.

in activation of  $\text{H}_2\text{O}_2$ . On the other hand, the double mutant F43Y/H64D Mb showed a  $K_{\text{m}}$  value of 0.44 mM, which is  $\sim 4.75$ -fold and  $\sim 4$ -fold lower than that of F43Y Mb and H64D Mb, respectively. These results indicate that the replacement of His64 with an Asp in F43Y Mb facilitates the binding of indole to the heme active site, by combination of the effect of both mutations. As a result, F43Y/H64D Mb exhibited a catalytic efficiency ( $k_{\text{cat}}/K_{\text{m}} = 198 \text{ M}^{-1} \text{ s}^{-1}$ )  $\sim 1.8$ -fold and  $\sim 4.2$ -fold higher than that of the single mutant F43Y Mb and H64D Mb, respectively (Table 1). Notably, it is also slightly higher ( $\sim 1.16$ -fold) than that of the triple mutant H64D/V68I/I107V Mb,  $170 \text{ M}^{-1} \text{ s}^{-1}$ , the highest catalytic efficiency reported by Watanabe and co-workers.<sup>23</sup>

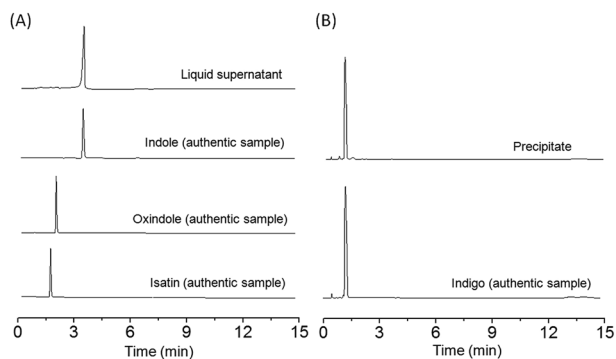
### HPLC analysis of the side products

In order to compare the yield and chemoselectivity of different Mb mutants for the indigo formation, we performed HPLC studies to measure the amounts of the indigo product and other side products, such as oxindole and isatin according to the proposed mechanism by Watanabe and co-workers (Scheme S1<sup>†</sup>).<sup>23</sup> To simplify the determination, we divided the reaction mixture into two fractions by centrifugation, *i.e.*, the supernatant and the blue precipitate, which were quantified by HPLC individually. As shown in Fig. 5 for F43Y Mb, the side products and the unreacted indole in the supernatant were extracted with chloroform, evaporated and re-dissolved in 50% methanol, and were monitored by HPLC using a wavelength of 280 nm (Fig. 5A). The blue precipitate was dissolved in DMF and monitored by HPLC at 250 nm (Fig. 5B). The authentic samples of indole, oxindole, isatin, and indigo were also monitored by HPLC for comparison. The results showed that a majority of the extracted components in supernatant was unreacted indole, with a slight amount of oxindole, isatin and other products (other areas) (Table 2), whereas most of the precipitate ( $\sim 95\%$ ) was the product indigo. Based on the consumed indole, the yield of indigo in reaction catalyzed by F43Y Mb was estimated to be 54%, which increased by  $\sim 170\%$  compared to the highest yield (20%) reported previously for both H64D Mb<sup>23</sup> and an enzymatic mimicking system of Fe(III)-porphyrin.<sup>24</sup> For the reaction catalyzed by F43Y/H64D Mb, less side product of



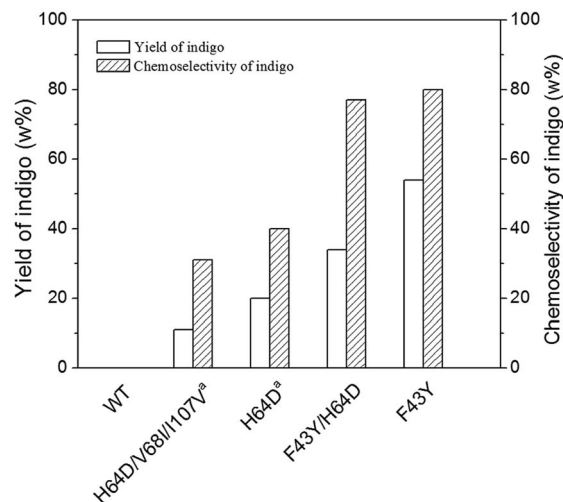
**Table 1** Kinetic parameters for H<sub>2</sub>O<sub>2</sub>-dependent oxidation of indole producing indigo catalyzed by WT Mb and its mutants

Mbs	$k_{\text{cat}}$ (min <sup>-1</sup> )	$K_m$ (mM)	$k_{\text{cat}}/K_m$ (M <sup>-1</sup> s <sup>-1</sup> )
WT Mb	n.d.	n.d.	n.d.
F43Y Mb	13.8 ± 1.2	2.10 ± 0.37	110
F43Y/H64D Mb	5.22 ± 0.13	0.44 ± 0.05	198
H64D Mb <sup>23</sup>	4.8	1.7	47
H64D/V68I/I107V Mb <sup>23</sup>	39	3.9	170

**Fig. 5** HPLC analysis of (A) the components extracted from the liquid supernatant of reaction mixture and monitored at 280 nm, and (B) the precipitate monitored at 250 nm catalyzed by F43Y Mb. HPLC traces of authentic samples of oxindole, isatin and indigo were shown for comparison.

oxindole, a similar amount of isatin, and a larger amount of unknown side products were produced (Fig. S6†), which resulted in a relative low yield of indigo (34%) compared to the single mutant F43Y Mb (Table 2).

Similar to the observations for both F43Y Mb and F43Y/H64D Mb, Watanabe and co-workers showed that H64D Mb and its mutants, such as H64D/V68I/I107V Mb, all produced oxindole and isatin, as well as other unknown side products, in the oxidation of indole.<sup>23</sup> It was proposed that indole was first oxidized in the heme active site of Mb upon activation by H<sub>2</sub>O<sub>2</sub>, generating indoxyl, and further oxidized to a radical species, followed by the radical coupling reaction that produces the product of indigo (Scheme S1†).<sup>23</sup> Moreover, the side products were proposed to be generated by direct oxidation of indole to oxindole, oxidation of the radical species to isatin, or other coupling reactions. The results in Table 2 suggested that the mutation in the heme distal pocket affects the radical coupling efficiency of indoxyl, thus leading to different yields of indigo. Based on these results, the chemoselectivity of indigo formation

**Fig. 6** Comparison of the yield and chemoselectivity of indigo catalyzed by WT Mb and its mutants (a, ref. 23).

was also estimated. As shown in Fig. 6, F43Y Mb was found to exhibit a chemoselectivity of ~80%, which is ~10% higher than that of F43Y/H64D Mb, and is ~100% higher than that of H64D Mb (40%), the highest reported in previous study.<sup>23</sup> These observations indicate that the introduction of Tyr43 to the heme distal site, especially for the formation of Tyr-heme cross-link, can increase the coupling efficiency of indoxyl radical and thus improve the yield of indigo.

### Use of biosynthesized indigo as a textile dye

Due to the low solubility of indigo in pure water, we found that the commercial product of indigo can hardly be used directly as a dye. In current industrial process, indigo is reduced to the water-soluble leuco form by an excess of reducing agent such as sodium dithionite, which, however, produces pollutants of sulfate and sulfite by decomposition.<sup>25</sup> As shown in Fig. 7a and b, when a white cotton textile directly dyed with indigo–water mixture, a non-uniform blue color was appeared. On the other hand, inspired by the good dispersion of the biosynthesized indigo after the reaction (Fig. 2A), we envisaged that it might be able to directly use the biosynthesized indigo in the reaction solution as a dye. Therefore, we tested for a white cotton textile by soaking in the solution for 2 h at 37 °C, and the resultant cotton textile appeared light blue (Fig. 7c). To improve the dyeing effect, we soaked the white cotton textile in the solution containing indole and F43Y Mb before initiating the reaction by addition of H<sub>2</sub>O<sub>2</sub>. After dyeing for 2 h, the cotton textile showed a blue color (Fig. 7d), suggesting a better dyeing effect compared

**Table 2** The amounts of indigo, side products and unreacted indole after 15 min reaction catalyzed by Mb mutants and estimated by HPLC

Mb mutants	Indigo (μM)	Oxindole (μM)	Isatin (μM)	Indole (μM)	Other areas	Indigo yield
F43Y Mb	180	31	59	332	0.021	54%
F43Y/H64D Mb	120	10	60	292	0.084	34%
H64D <sup>23</sup>	36	21	34	643	0.16	20%
H64D/V68I/I107V Mb <sup>23</sup>	34	31	46	448	0.18	11%





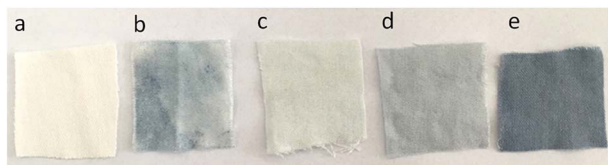


Fig. 7 A white cotton textile (a), dyed with commercial indigo product (b), soaked in the biosynthesized indigo solution after reaction for 2 h (c), (d) soaked in the solution before reaction and kept for 2 h, and (e) sprayed with concentrated indigo solution after reaction.

to that by dyeing after reaction (Fig. 7c). This observation could be attributed to a water-soluble intermediate, indoxyl, that was generated during the reaction (Scheme S1†).<sup>23</sup> Therefore, the biosynthesis of indigo may occur on the surface of cotton textile, resulting in an uniform blue color. Moreover, we found that the blue cotton textile can be further dyed to dark blue by spraying the concentrated biosynthesized indigo on the surface (Fig. 7e). These results suggest that a convenient and green dyeing method could be established, that is, dyeing a cotton textile during the biosynthesis of indigo, followed by further spraying the concentrated indigo product. More importantly, this method is a green method, without the need of strong acids/bases or any reducing agents, which is thus superior to the current industrial dyeing method.<sup>30</sup>

## Conclusions

In summary, we showed that the F43Y Mb mutant with a Tyr-heme cross-link can efficiently catalyze the oxidation of indole to indigo, with a yield as high as 54% compared to the highest yield of ~20% reported to date in literature. By further modifying the heme active site, the double mutant F43Y/H64D Mb exhibited the highest catalytic efficiency of the reported artificial enzymes designed in Mb. Moreover, both F43Y Mb and F43Y/H64D Mb produced indigo with a chemoselectivity as high as ~80%. In addition, we established a convenient and green dyeing method based on the reaction system, without the need of strong acids/bases or any reducing agents, which was successfully applied to dye a white cotton textile with satisfied blue color. Therefore, we expect the current artificial enzymes and dyeing method to have practical applications in the future.

## Materials and methods

### Protein preparation

WT (wild-type) sperm whale Mb was expressed in BL21(DE3) cells using the Mb gene of pMbt7-7, where the position of 123 is Asp (D), different from that of Asn (N) as reported by Springer and Sligar,<sup>31</sup> and purified as described previously.<sup>32</sup> F43Y Mb and F43Y/H64D Mb protein were expressed in BL21(DE3) cells and purified using the procedure described previously.<sup>26</sup>

### Kinetic UV-Vis studies of indigo formation

Kinetic UV-Vis studies of indigo formation catalyzed by F43Y Mb and F43Y/H64D Mb were performed on a Hewlett-

Packard 8453 diode array spectrometer. Control study of WT Mb was performed under the same conditions. Protein concentrations were determined with an extinction coefficient of  $\epsilon_{409\text{nm}} = 157 \text{ mM}^{-1} \text{ cm}^{-1}$  for WT Mb,<sup>31</sup>  $\epsilon_{403} = 146 \text{ mM}^{-1} \text{ cm}^{-1}$  for F43Y Mb, and  $\epsilon_{404} = 140 \text{ mM}^{-1} \text{ cm}^{-1}$  for F43Y/H64D Mb, respectively, as calculated using the standard hemochromogen method.<sup>33</sup> The reaction was carried out in 50 mM potassium phosphate buffer (pH 7.4) containing 0.5–4 mM indole, 10  $\mu\text{M}$  protein, with a final volume of 2 mL. The mixture was first incubated at 37 °C for 30 minutes, followed by an addition of  $\text{H}_2\text{O}_2$  (1 mM) to initiate the reaction. The reaction was monitored by the absorbance change at 670 nm ( $\epsilon = 4.8 \text{ mM}^{-1} \text{ cm}^{-1}$ ),<sup>23</sup> due to the formation of the indigo product. The initial rates *versus* substrate concentrations were fitted using the Michaelis-Menten equation to obtain the kinetic parameters.

### Analysis of the reaction mixture after oxidation reaction

The mixture containing 1 mM indole, 20  $\mu\text{M}$  F43Y Mb mutant, 1 mM  $\text{H}_2\text{O}_2$  in a final volume of 3 mL was reacted at 37 °C for 15 min. Then the reaction mixture was centrifuged at 4000 r/min for 30 min, which generated blue precipitates and light yellow supernatant. The precipitate was dissolved in a mixture of methanol and water (1 : 1, v/v), which was then applied to a thin-layer plate of silica gel G (0.2 mm  $\times$  40 mm  $\times$  70 mm) and developed with  $\text{CHCl}_3/\text{CH}_3\text{OH}$  (50 : 1, v/v).<sup>4</sup> The UV-Vis spectrum of the precipitate was recorded by dissolving in DMF. The mass spectrum of was determined on G2-XS QTOF mass spectrometer (Waters). The precipitate-DMF solution was mixed with 1% formic acid and transferred into the mass spectrometer chamber for measurement under the negative mode.

**HPLC analysis of the liquid supernatant.** The liquid supernatant was extracted with chloroform. The organic layer was separated, evaporated and redissolved in a 1 : 1 mixture of methanol and water, then an aliquot of this mixture was injected to a 2.1  $\times$  100 mm BEH C18 1.7  $\mu\text{M}$  UPLC column, which was eluted with the same buffer at a flow rate of 0.2 mL min<sup>-1</sup> at 35 °C, and the eluent was monitored at 280 nm. Determination of 0.5 mM authentic indole, 1 mM authentic oxindole, 1 mM authentic isatin were performed in the same liquid phase conditions. The concentrations of produced isatin, oxindole and remaining indole were then calculated. The yield of indigo was calculated based on the consumed indole as follows:<sup>23</sup>  $[\text{indigo}] \times 2 / [\text{consumed indole}] \times 100\%$ . Moreover, the chemoselectivity of indigo formation was also estimated as follows:<sup>23</sup>  $[\text{indigo}] / ([\text{indigo}] + [\text{isatin}] + [\text{oxindole}]) \times 100\%$ .

**HPLC analysis of the precipitation.** The precipitation was redissolved in DMF, producing a blue solution, and an aliquot of this blue solution was injected to a 2.1  $\times$  100 mm BEH C18 1.7  $\mu\text{M}$  HPLC column. The column was eluted with a 1 : 1 mixture of methanol and water at a flow rate of 0.2 mL min<sup>-1</sup> at 35 °C, and the eluent was monitored at 250 nm. Determination of 0.5 mM authentic indigo was performed in the same liquid phase conditions, and the concentration of produced indigo was calculated.



## Use of biosynthesized indigo as a textile dye

To use the biosynthesized indigo as a textile dye, we tested three methods. The first was to soak a white cotton textile for 2 h in the reaction solution, after oxidation of indole (3 mM) for 15 min at 37 °C, as catalyzed by F43Y Mb (20 μM) and H<sub>2</sub>O<sub>2</sub> (1 mM). The second one was to soak in the solution containing indole (3 mM) and F43Y Mb (20 μM) before initiating the reaction by addition of H<sub>2</sub>O<sub>2</sub> (1 mM) for 15 min at 37 °C, followed by further dyeing for additional 2 h. The third one was on the basis on the second, by spraying the concentrated biosynthesized indigo on the surface of cotton textile, then dried in air. A control experiment was performed by using the commercial product of indigo, with a mixture of indigo–water (3 g L<sup>−1</sup>), and dyeing at 37 °C for 2 h.

## Conflicts of interest

There are no conflicts to declare.

## Acknowledgements

It is a pleasure to acknowledge Prof. S. G. Sligar and Prof. Y. Lu of University of Illinois at Urbana-Champaign, for the kind gift of sperm whale Mb gene. This work was supported by the National Science Foundation of China, NSFC (31370812; 21701081).

## References

- 1 B. D. Ensley, B. J. Ratzkin, T. D. Osslund, M. J. Simon, L. P. Wackett and D. T. Gibson, *Science*, 1983, **222**, 167–169.
- 2 E. S. Ferreira, A. N. Hulme, H. McNab and A. Quye, *Chem. Soc. Rev.*, 2004, **33**, 329–336.
- 3 L. Wolf, *Chem. Eng. News*, 2011, **89**, 44.
- 4 C. S. W. Koehler, *Today's Chemist at Work*, 1999, **8**, 85–99.
- 5 Q. S. Li, U. Schwaneberg, P. Fischer and R. D. Schmid, *Chemistry*, 2000, **6**, 1531–1536.
- 6 K. Nakamura, M. V. Martin and F. P. Guengerich, *Arch. Biochem. Biophys.*, 2001, **395**, 25–31.
- 7 H. M. Li, L. H. Mei, V. B. Urlacher and R. D. Schmid, *Appl. Biochem. Biotechnol.*, 2008, **144**, 27–36.
- 8 T. Mouri, N. Kamiya and M. Goto, *Biochem. Eng. J.*, 2011, **53**, 229–233.
- 9 Y. Lu, N. Yeung, N. Sieracki and N. M. Marshall, *Nature*, 2009, **460**, 855–862.
- 10 Y. Lin, J. Wang and Y. Lu, *Sci. China: Chem.*, 2014, **57**, 346–355.
- 11 T. Ueno, S. Abe, N. Yokoi and Y. Watanabe, *Coord. Chem. Rev.*, 2007, **251**, 2717–2731.
- 12 Y.-B. Cai, X. H. Li, J. Jing and J.-L. Zhang, *Metallomics*, 2013, **5**, 828–835.
- 13 K. Oohora and T. Hayashi, *Curr. Opin. Chem. Biol.*, 2014, **19**, 154–161.
- 14 I. D. Petrik, J. Liu and Y. Lu, *Curr. Opin. Chem. Biol.*, 2014, **19**, 67–75.
- 15 Y.-B. Cai, S.-Y. Yao, M. Hu, X. Liu and J.-L. Zhang, *Inorg. Chem. Front.*, 2016, **3**, 1236–1244.
- 16 Z.-H. Shi, K.-J. Du, B. He, S.-Q. Gao, G.-B. Wen and Y.-W. Lin, *Inorg. Chem. Front.*, 2017, **4**, 2033–2036.
- 17 Y.-W. Lin, *Coord. Chem. Rev.*, 2017, **336**, 1–27.
- 18 Y.-W. Lin, *Arch. Biochem. Biophys.*, 2018, **641**, 1–30.
- 19 S. Hirota and Y.-W. Lin, *J. Biol. Inorg. Chem.*, 2018, **23**, 7–25.
- 20 Y. Yu, C. Hu, L. Xia and J. Wang, *ACS Catal.*, 2018, **8**, 1851–1863.
- 21 L.-L. Yin, H. Yuan, K.-J. Du, B. He, S.-Q. Gao, G.-B. Wen, X. Tan and Y.-W. Lin, *Chem. Commun.*, 2018, **54**, 4356–4359.
- 22 A. Bhagi-Damodaran, J. H. Reed, Q. Zhu, Y. Shi, P. Hosseinzadeh, B. A. Sandoval, K. A. Harnden, S. Wang, M. R. Sponholtz, E. N. Mirts, S. Dwaraknath, Y. Zhang, P. Moenne-Loccoz and Y. Lu, *Proc. Natl. Acad. Sci. U. S. A.*, 2018, **115**, 6195–6200.
- 23 J. Xu, O. Shoji, T. Fujishiro, T. Ohki, T. Ueno and Y. Watanabe, *Catal. Sci. Technol.*, 2012, **2**, 739–744.
- 24 S. L. H. Rebelo, M. Linhares, M. M. Q. Simões, A. M. S. Silva, M. G. P. M. S. Neves, J. A. S. Cavaleiro and C. Freire, *J. Catal.*, 2014, **315**, 33–40.
- 25 T. M. Hsu, D. H. Welner, Z. N. Russ, B. Cervantes, R. L. Prathuri, P. D. Adams and J. E. Dueber, *Nat. Chem. Biol.*, 2018, **14**, 256–261.
- 26 D.-J. Yan, W. Li, Y. Xiang, G.-B. Wen, Y.-W. Lin and X. Tan, *ChemBioChem*, 2015, **16**, 47–50.
- 27 D.-J. Yan, H. Yuan, W. Li, Y. Xiang, B. He, C.-M. Nie, G.-B. Wen, Y.-W. Lin and X. Tan, *Dalton Trans.*, 2015, **44**, 18815–18822.
- 28 L.-L. Li, H. Yuan, F. Liao, B. He, S.-Q. Gao, G.-B. Wen, X. Tan and Y.-W. Lin, *Dalton Trans.*, 2017, **46**, 11230–11238.
- 29 L.-L. Yin, H. Yuan, C. Liu, B. He, S.-Q. Gao, G.-B. Wen, X. Tan and Y.-W. Lin, *ACS Catal.*, 2018, **8**, 9619–9624.
- 30 R. S. Blackburn, T. Bechtold and P. John, *Color. Technol.*, 2009, **125**, 193–207.
- 31 B. A. Springer and S. G. Sligar, *Proc. Natl. Acad. Sci. U. S. A.*, 1987, **84**, 8961–8965.
- 32 J. A. Sigman, B. C. Kwok and Y. Lu, *J. Am. Chem. Soc.*, 2000, **122**, 8192–8196.
- 33 M. Morrison and S. Horie, *Anal. Biochem.*, 1965, **12**, 77–82.

